On the Effect of Trailing-Edge Bluntness on Airfoil Noise

Basim Al Tlua *[1] and Joana Rocha †[2]
[1]Department of Mechanical and Aerospace Engineering, Carleton University, Ottawa, Canada

Résumé

Le but de cette étude est d'étudier expérimentalement l'effet du profil aerodynamique sur la génération de bruit tonal à différents angles d'attaque et à des nombres de Reynolds allant de faibles à modérés. Des mesures aéroacoustiques détaillées sont effectuées pour un profil aérodynamique, à trois angles d'attaque : 0°, 5° et 10°. Les nombres de Reynolds basés sur la corde du profil aérodynamique analysés sont 2.8×10^5, 3.7×10^5 et 5×10^5, correspondant à des vitesses de flux libre de 14, 18 et 24 m/s, respectivement. On voit que le bruit du profil aérodynamique avec un bord de fuite droit passe de bruit large bande à un bruit tonal intensif pour un angle d'attaque croissant ; tandis qu'il passe de bruit tonal à bruit large bande avec un nombre de Reynolds croissant. De plus, les résultats montrent que pour des valeurs plus élevées des nombres de Reynolds, le pic tonal dominant diminue en amplitude et se déplace vers des fréquences plus élevées. En général, on observe qu'à mesure que la netteté du bord de fuite augmente, les pics tonals dominants ont des amplitudes globales plus grandes.

Mots clés: bruit de profil aérodynamique, épaisseur du bord de fuite.

Abstract

The purpose of this study is to experimentally investigate the effect of trailing edge bluntness on the generation of airfoil tonal noise at different angles of attack and low to moderate Reynolds numbers. Detailed aeroacoustic measurements are made for an airfoil at three angles of attack: 0°, 5°, and 10°. Airfoil chord-based Reynolds numbers analyzed are 2.8×10^5, 3.7×10^5 and 5×10^5, corresponding to free stream velocities of 14, 18 and 24 m/s, respectively. The airfoil noise with a straight trailing edge is seen to change from a broadband hump to intensive tonal noise with increasing angle of attack, while it changes from tonal noise to a broadband hump with increasing Reynolds number. Moreover, results show that for higher values of Reynolds numbers the dominant tonal peak decreases in amplitude and shifts to higher frequencies. In general, it is observed that as the trailing edge bluntness increases, the dominant tonal peaks have larger overall amplitudes.

Keywords: airfoil noise, trailing edge bluntness.

1 Introduction

Airfoil trailing edge (TE) noise is believed to be a major noise source in many industrial applications, such as wind turbines, high lift devices on aircraft airframes, cooling fan blades, to name a few. The character and level of trailing edge self-noise are known to be highly sensitive to Reynolds number (free stream velocity), angle of attack (AoA), airfoil geometry and trailing edge bluntness [1]. TE noise has a characteristic narrowband structure consisting of a broadband hump superimposed with many tones, at low Reynolds numbers, with minor residue turbulence in the free stream [2, 3]. In contrast, for high Reynolds number flow, TE noise is typically broadband in nature. If the chord length of the airfoil is larger than the acoustic wavelength, the convective turbulent eddies in the boundary layer will scatter effectively into "broadband noise" at the TE. In the situation of Reynolds number of $2.8\times10^5 \leq Re_c \leq 5\times10^5$ the boundary layer on the airfoil surface is laminar, or in transition, but potentially unstable. Under a certain range of conditions, hydrodynamic instabilities such as the Tollmien–Schlichting (T–S) waves, grow in the boundary layer and eventually scatter into noise at the trailing edge. This mechanism of self-noise is referred to as instability tonal noise. Tam [4] proposed that the tonal noise was generated by a feedback loop between the oscillating wake and the airfoil trailing edge. After a moderate Reynolds number is reached, a nominal two-dimensional vortex shedding will be formed downstream of a blunt TE from which narrowband tonal noise will be emitted from the shear layer [5, 6]. It is worth mentioning that the use of blunt TE could also reduce the base pressure and subsequently increase the base drag. At moderate angle of attack, flow separates near the TE on the suction side of the airfoil to produce TE self-noise; at large angle of attack, large scale separation occurs causing the airfoil to radiate low frequency noise from the chord as a whole.

Previous studies on a NACA-0012 airfoil have shown that the prerequisite condition for a broadband hump and/or tones to occur is the existence of a separation region near the trailing edge on the pressure surface [7, 8]. It was concluded that the incoming T–S waves must be amplified by the separating shear layer before tonal noise can be radiated effectively. For most symmetrical airfoils, an adverse pressure gradient always prevails at the rear region of the airfoil, and its level depends on the airfoil's profile and angle of attack. These factors influence the separation region, which

* BasimAlTlua@cmail.carleton.ca
† Joana.Rocha@carleton.ca

ultimately affects the intensity and frequency of the radiated instability tonal noise.

Through the use of different degrees of TE bluntness, this study aims to investigate whether flow separation can be reduced or prevented, hence providing a reduction in tonal noise. The ability to produce a turbulent wake by the trailing edge could potentially eliminate or reduce the tonal noise source. It is hoped that results from this study can be used to provide aid in the design of low noise airfoils suitable for low to moderate Reynolds number flows.

2 Experimental setup

2.1 Airfoil model and trailing edge design

The airfoil under investigation is a NACA-0012 airfoil with different level of TE bluntness, as shown in Figure 1. The airfoil model with the straight trailing edge (S0) is used as the reference configuration for all tests and so will be referred to as the baseline. The chord length of the S0 airfoil is 300 mm, and the width is 510 mm. Between the leading-edge x/c=0 and x/c=0.73, the original airfoil model profile is unmodified, where x is the streamwise direction. Further downstream, $0.73 \leq x/c \leq 1.0$, is a section that can be removed and replaced by either a straight (S0) or modified trailing edge profiles (S1 and S2). Once attached, the trailing edge section forms a continuous profile. Boundary layer tripping elements were applied using rough sandpaper near the leading edge on both sides of the airfoil at x/c = 0.15.

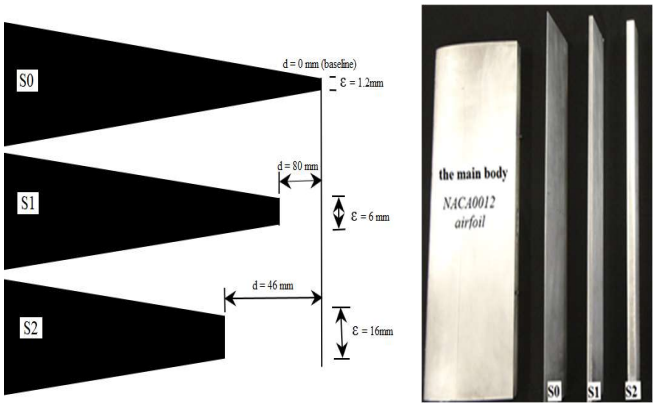

Figure 1: Airfoil model with three different degrees of TE bluntness

Trailing edge noise measurements for a NACA-0012 airfoil model are presented. Far-field noise spectra is obtained using a directional calibrated microphone. Treatments were applied to the trailing edge of the airfoil to modify its thickness and to model different blunt trailing edges. Three trailing edge configurations were examined with the level of thickness "ε" as shown in Table 1. The airfoil was placed at angles of attack ranging from 0° to 10°.

2.2 Wind tunnel facility

The experiment was conducted in a closed-loop type, low speed wind tunnel at the Carleton University. The wind tunnel contains an exit cross-section that is rectangular and has dimensions of 0.3 m (height) × 0.73 m (span). The airfoil was mounted vertically across the entire width of the test section, as shown in Figure 2. Taking into account the maximum velocity achievable by the current wind tunnel, a Reynolds number of 2.8×10^5 (freestream velocity, U_∞, of 14 m/s), 3.7×10^5 (U_∞=18 m/s) and 5×10^5 (U_∞ = 24 m/s) were chosen for this study. Further details can be found in [9,10].

Table 1: Airfoil trailing edge configurations.

Model	c [mm]	d [mm]	ε [mm]
S0	300	0	1.2
S1	220	80	6
S2	254	46	16

Figure 2: Wind tunnel at Carleton University.

2.3 Instruments and procedures

To measure the radiated self-noise from the airfoil, a single calibrated microphone (Bruel & Kjaer 4944-A, ¼ inch) at a polar angle of θ = 90°, is mounted at a distance of 1.4 m perpendicular to the airfoil trailing edge at mid-span, as shown in Figure 3.

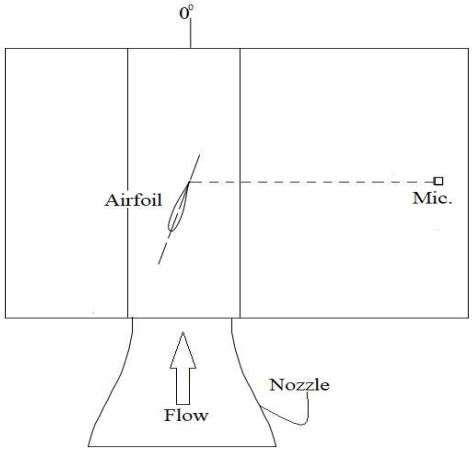

Figure 3: Schematic showing the position of the microphone in the test section.

Microphone signals were amplified by a B&K Nexus amplifier before digitally stored in a computer, through an A/D converter of 24-bit resolution. Acoustic data was sampled at 20 kHz and recorded for 30 seconds. The digitized data was passed through a time domain filter to remove low and high frequency contamination, caused by the microphone's low frequency roll off and high-frequency aliasing. The band-pass

filter used is a Butterworth filter with the first and second stopband frequencies of 100 and fs/2 Hz, respectively, where fs is the sampling frequency. The attenuation is 60 dB for both the first and second stopband. The passband ripple was kept as the 1 dB default and the band match used was a stopband. The sound pressure level, SPL, is computed using the root mean square (RMS) of filtered pressure using the following equation:

$$SPL = 10\, log_{10}\left(p^2_{RMS}/P^2_{ref}\right)$$

where P_{ref} is the standard reference pressure in air, 20 µPa. The background noise of the facility, i.e., an empty test section without the presence of the airfoil model, was measured prior and after the airfoil noise study [10]. The ranges of flow speed and of angle of attack in which the tonal trailing edge noise of an airfoil is observed is a key step in the characterization. The first acoustic data was registered by simply listening to the sound for determining the limiting conditions of the tonal trailing edge noise. The measurements were conducted at several velocities (14, 18 and 24 m/s). It was found that the clean airfoil exhibited several regimes of tonal noise generation. This fact motivated the current detailed investigation. The registered data was transposed into SPL versus frequency for different angles of attack and flow velocities, as discussed in detail in the following section.

3 Result

This section surveys and discusses the experimental results for the NACA-0012 airfoil. The detailed investigation of the noise emission and its dependence on the tripping, angle of attack, and TE bluntness is discussed. It is observed that the separation bubble is a necessary condition for the existence of high-intensity trailing-edge noise. Comparison with previous studies provides reasonable agreement and confirms that the measurements are reliable. Lowson et al. [11] examined NACA-0012 and NACA-23015 airfoils. They suggested the involvement of a separated flow in the noise model. In their model, it is proposed that the T-S waves were strongly amplified by the shear layer in the laminar separation. They also outlined a region of conditions (with respect to Re and angle of attack) where tonal noise is expected to occur for the NACA-0012 airfoil. Later in Probsting et al. [12], an overall figure was compiled showing this region and summarizing results of several studies examining different points in and outside of the region. This is shown in Figure 4. Many experimental observations tend to fall in between a bell-shaped envelope (Figure 4), as already reported by Desquesnes et al. [13], where tonal noise has often been observed (solid symbols). Data for the present study comprises relatively low to moderate Reynolds numbers ($Re_c = 2.8 \times 10^5 - 5 \times 10^5$) and the measurement points are indicated (in black squares). The reduction of tonal noise for lower Reynolds numbers at AoA = 4° is corroborated by the data by, Nash, Lowson and McAlpine [14] and the low-Reynolds-number limit of Desquesnes et al. [13]. When the Reynolds number is increased, separation and transition to turbulence tend to occur further upstream on both the suction and pressure sides, which is

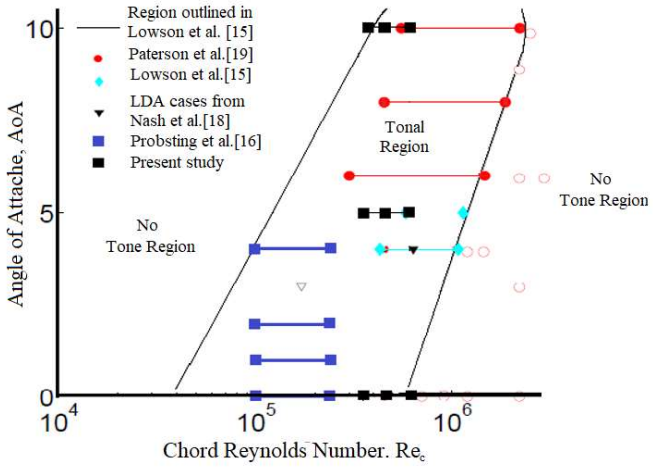

Figure 4: Region of Reynolds number and angle of attack where tonal noise can be found for a NACA-0012 Airfoil. Adapted from Probsting et al. [12].

considered the cause for the suppression of tonal noise. Instead, in this regime the acoustic emissions from the airfoil are of broadband nature (Paterson et al. [15]). At zero angle of attack this limit is reached at a Reynolds number of approximately 500,000 for the NACA-0012 at the lower limit, and transition will not occur upstream of the trailing edge. Instead, a laminar boundary layer and vortex shedding behind the trailing edge might result in weak or no tonal noise. Figure 5 shows the sound pressure level radiated by the straight airfoil for three different velocities (14, 18 and 24 m/s) corresponding to Reynolds numbers of 2.8×10^5, 3.7×10^5 and 5×10^5, respectively, at angle of attack of 0°. Results shown in Figure 5 are following discussed, in section 3.1.

3.1 Far field noise

The far-field spectra for the three velocities investigated illustrate the behavior of the NACA-0012 airfoil, as shown in Figure 5 for AoA 0^0. At 14 m/s a dominant tone at 351.6 Hz is clearly noticeable followed by two lower tones at 455.8 Hz and 555.9 Hz. At 18 m/s the hump is more visible with a marked dominant tone at 545.9 Hz. An interesting observation is the disappearance of the tones at 24 m/s. It is suspected that one or more of the components leading to tonal trailing edge noise such as instability waves, feedback loop or separation bubble is suppressed when velocity is increased to 24 m/s. It is observed that the frequency of the tone increases gradually with increasing velocities, and the tone intensity increases first to a maximum value and then decreases with the velocity. It is also found that the instability noise spectra changes from intensive tonal noise to broadband humps with increasing velocity.

Figure 6 shows the sound pressure level for the straight TE airfoil for various angles of attack, at a Reynolds number of $5x10^5$. It can be observed that there is no distinct tonal noise at 0°, while the spectrum exhibits 3 broadband humps at 5° between ~300 Hz and ~600 Hz. At AoA of 10° the instability noise exhibits an intensive tone at around 449.2 Hz followed by other tow lower tones at 527.3 Hz and 525 Hz.

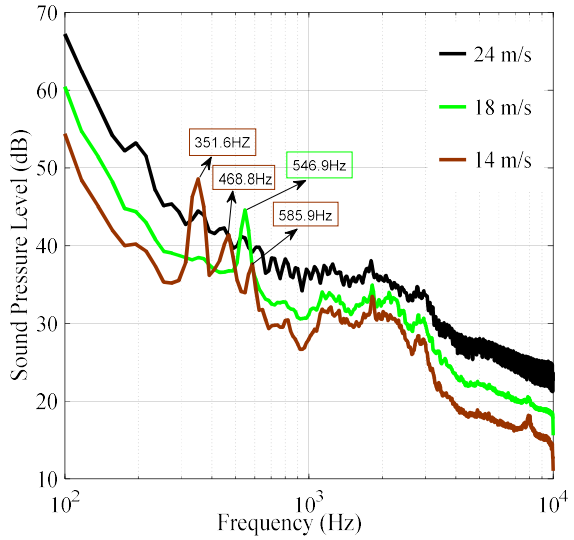

Figure 5: SPL radiated by the straight TE airfoil at 0° AoA, for various inflow velocities.

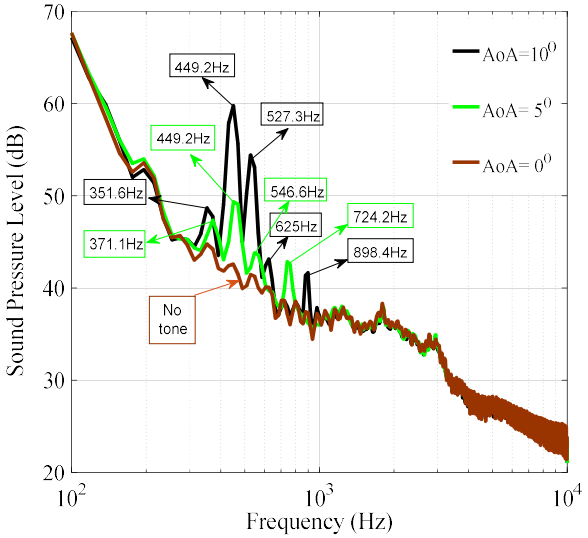

Figure 6: SPL radiated by the straight airfoil for various angles of attack, at a Reynolds number of 5×10^5 ($U_\infty = 24$ m/s).

In addition, high harmonic instability noise with much lower sound level is also found for angles of attack of (5°) at 724.2 Hz and for (10°) at 898.4 Hz. Overall, the instability noise changes from a broadband hump to intensive tonal noise with increasing angle of attack, but the main tone frequency does not change significantly with the angle of attack.

3.2 Influence tripping the flow

Figures 7(a) and 7(b) show the SPL for the straight trailing edge measure at 5° AoA, for the untripped and tripped flow cases, respectively. The spectrum for the untripped case is characterized by numerous tones for the deferent free stream velocities (Figure 7(a)). On the other hand, no tones are present for the tripped case (Figure 7(b)), in which broadband self noise is the dominant mechanism [16]. Boundary layers at both the suction and pressure surfaces are turbulent near the trailing surfaces. Without tripping, the boundary layer at

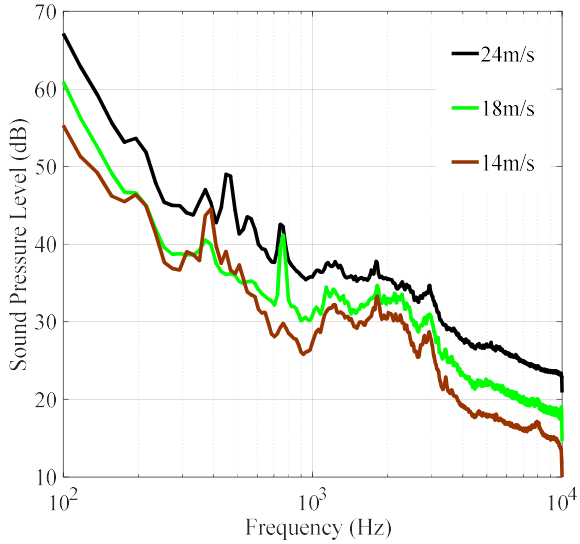

Figure 7(a): SPL measured at 5° AoA for U_∞ = 14,18 and 24 m/s, for the untripped airfoil.

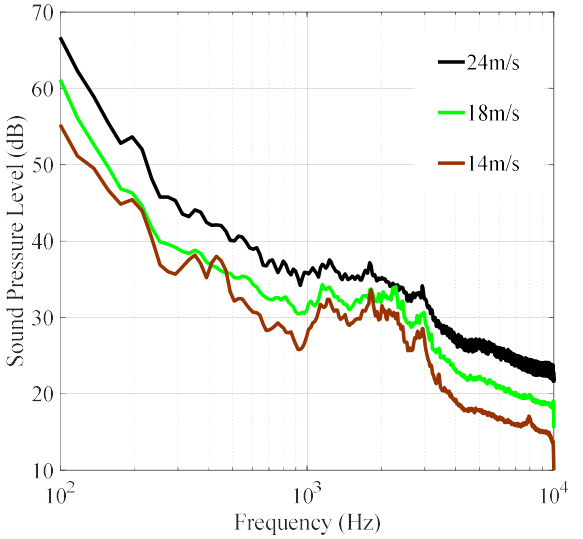

Figure 7(b): SPL measured at 5° AoA and U_∞= 14,18 and 24 m/s, for the tripped airfoil

the pressure surface is laminar (or separated) near the trailing edge.

3.3 Effect of TE bluntness

Measured spectra, including the effect of bluntness, are presented in Figure 8. The present analysis investigates the noise emitted by the three airfoils with different trailing edge bluntness tested at zero degree angle of attack (shown in Figure 1) – case in which the boundary layer flow is attached nearly all the way to the trailing edge of the airfoil. All the flow separation features tend to increase the complexity of the tone generation processes (present at higher AoA). In Figure 8 (a), for S0, one can observe a defined dominant tone. One can also notice that, for an increased flow velocity, the dominant tonal peak decreases in level and shifts to higher frequencies. On the other hand, Figure 8 (b) for S1 shows that as velocity of the flow is increased the dominant tonal peak increases in level and shifts to higher frequencies.

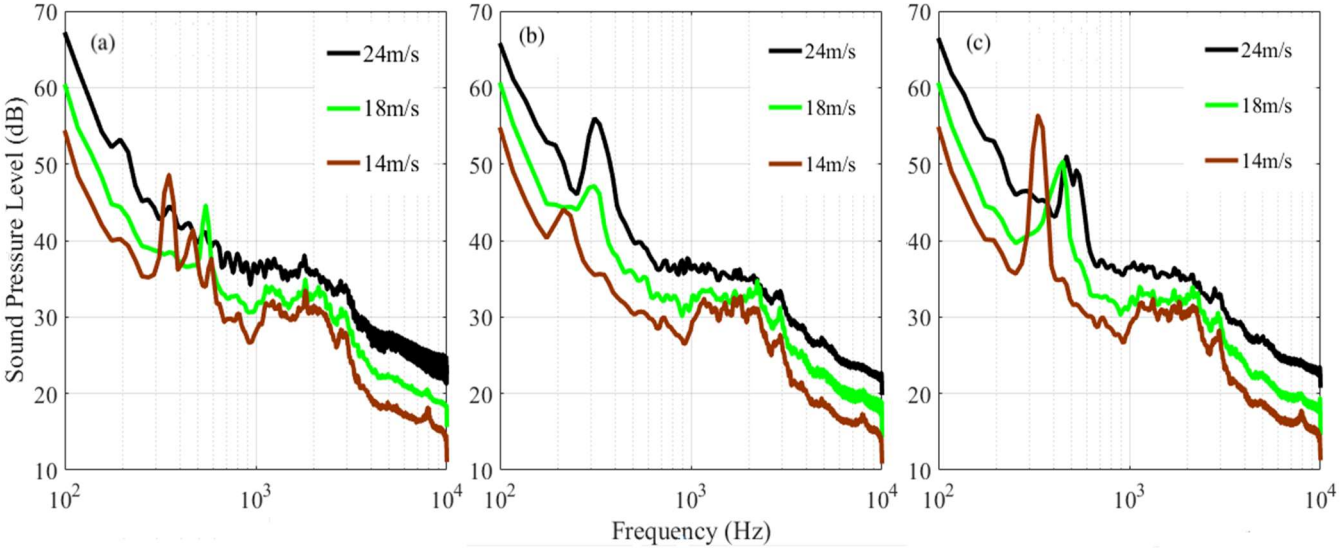

Figure 8: Effect of TE bluntness, for three TE configurations: (a) S0, (b) S1 and (c) S2. Results for 0° AoA , at14, 18 and 24 m/s.

For the S2 configuration, Figure 8 (c) shows three clearly defined tonal peaks for the lower Mach number case (Re = 2.8×10^5). One can also observe, for S0, that an increased Mach number, results into dominant tonal peak amplitude decrease, which disappears at 24 m/s. In general, it is observed that as the trailing edge bluntness increases, the dominant tonal peaks have larger overall amplitudes for the TE configurations analyzed.

3.4 Effect of the angle of attack

The effects of angle of attack of the airfoil model with different TE bluntness are shown in Figures 9 to 11. In Figure 9, as the angle of attack is increased, it is observed that although the spectral peak shifts to higher frequencies and its level decreases, the higher frequency fall-off portion of the spectra is seemingly invariant. This appearance is due to increased higher frequency contribution from the pressure side due to its thinner boundary layer thickness (with small turbulence scales). Still, the levels and the dependence on angle of attack basically agree. The results obtained with increased bluntness at the TE are presented in Figures 9, 10, and 11 for ε = 1.2, 6, and 16 mm, respectively. It is observed that the lower frequency behavior with changes in angle-of-attack appears to be little affected by the bluntness differences. However, the noise spectral peaks, which become more prominent with decreased bluntness, are effectively affected by angle of attack. The larger the angle, the more reduced the spectral peaks. Tonal noise scales with free stream velocity and frequency. It also depends on how TE bluntness compares to the boundary layer thickness [17], as well as on TE geometric features that determine flow angulation in the separated region aft of the TE. As shown in Figure 11, for a small AoA of 5°, the larger thickness produces higher SPL at lower frequency. Decreasing the thickness, ε, results in an increase of the tonal frequency. Also, tonal noise levels diminish, and spectra broaden since ε decreases compared to the boundary layer thicknesses. For the larger AoA of 10° (as in Figures 9, 10 and 11), the boundary layer thicknesses in the pressure side of the airfoil decrease, which leads to decreased levels of the tonal noise.

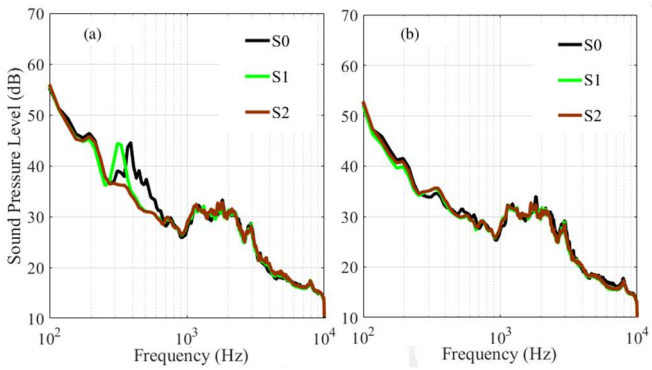

Figure 9: Effect of angle of attack for tests at U∞==14 m/s, for: (a) AoA = 5°, (b) AoA = 10°.

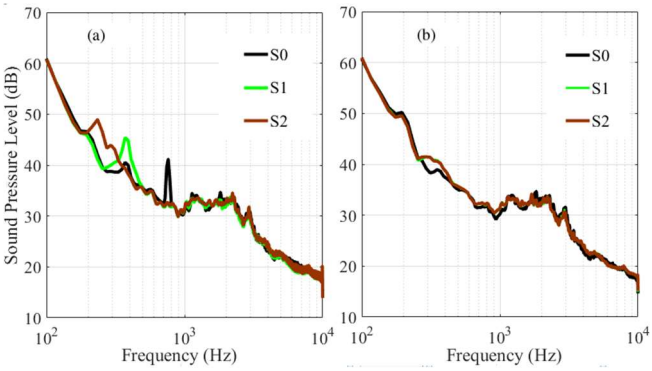

Figure 10: Effect of angle of attack for tests at U∞=18m/s, for: (a) AoA = 5°, (b) AoA = 10°.

4 Conclusion

The present work provides a detailed analysis of airfoil tonal noise generation at low Reynolds numbers. The effects of

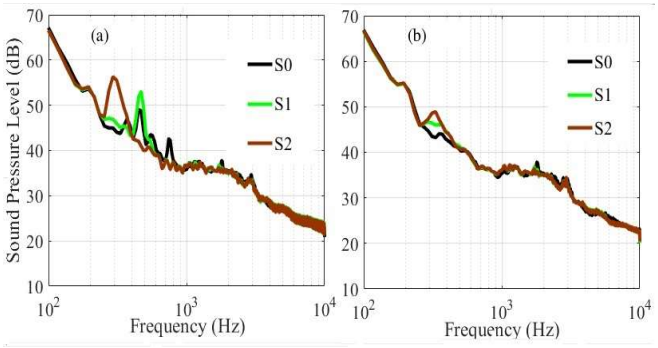

Figure 11: Effect of angle of attack for tests at U_∞=24 m/s, for: (a) AoA = 5°, (b) AoA = 10°.

trailing edge bluntness on noise generation and propagation over a NACA0012 airfoil with three different blunt trailing edge geometries are experimentally investigated for low to moderate Mach numbers. Far-field noise spectra is obtained using a single calibrated microphone. The effects of varying the free stream velocity and angle of attack on the far-field spectra are examined for TEs with different degrees of bluntness. The main findings of the present study include:

- For increased free stream velocity, the dominant tonal peak decreases in amplitude and shifts to higher frequencies.
- As the airfoil angle of attack is increased, the spectral peak shifts to higher frequencies and its amplitude decreases.
- In general, as the trailing edge bluntness increases, the dominant tonal peaks have larger amplitudes. For the same TE bluntenss, inceasing the flow velocity results into a shift of the dominant tonal peak to higher frequencies.

Acknowledgments

The author would like to thank his supervisor, Professor Joana Rocha, for all her guidance and support.

References

[1] Brooks TF, Pope DS, Marcolini MA. Airfoil self-noise and prediction. Washington, DC: National Aeronautics and Space Administration, Office of Management, Scientific and Technical Information Division; 1989 Jul 1.

[2] Williams JF, Hall LH. Aerodynamic sound generation by turbulent flow in the vicinity of a scattering half plane. Journal of fluid mechanics. 1970 Mar;40(4):657-70.

[3] Jones L, Sandberg R. Numerical investigation of airfoil self-noise reduction by addition of trailing-edge serrations. In16th AIAA/CEAS Aeroacoustics Conference 2010 Jun 7 (p. 3703).

[4] Tam CK. Discrete tones of isolated airfoils. The Journal of the Acoustical Society of America. 1974 Jun;55(6):117-7.

[5] Chong TP, Joseph PF, Gruber M. Airfoil self noise reduction by non-flat plate type trailing edge serrations. Applied Acoustics. 2013 Apr 1;74(4):607-13.

[6] Herr M. Design criteria for low-noise trailing-edges. In13th AIAA/CEAS Aeroacoustics Conference (28th AIAA Aeroacoustics Conference) 2007 May (p. 3470).

[7] Finez A, Jacob M, Jondeau E, Roger M. Broadband noise reduction with trailing edge brushes. In16th AIAA/CEAS aeroacoustics conference 2010 Jun (p. 3980).

[8] Geyer T, Sarradj E, Fritzsche C. Measurement of the noise generation at the trailing edge of porous airfoils. Experiments in fluids. 2010 Feb;48(2):291-308.

[9] Al Tlua B, Rocha J. Development and Testing of an Aeroacoustic Wind Tunnel Test Section. Canadian Acoustics. 2019 Oct 16;47(3):64-5.

[10] Al Tlua B, Rocha J. Optimization and Testing of Flat-Plate Trailing-Edge Serration Geometry for Reducing Airfoil Self-Noise. Canadian Acoustics. 2020 Dec 13;48(4):7-18.

[11] Lowson M, Fiddes S, Nash E. Laminar boundary layer aeroacoustic instabilities. In32nd Aerospace Sciences Meeting and Exhibit 1994 Jan (p. 358).

[12] Pröbsting S, Serpieri J, Scarano F. Experimental investigation of aerofoil tonal noise generation. Journal of Fluid Mechanics. 2014 May 25;747:656.

[13] Desquesnes G, Terracol M, Sagaut P. Numerical investigation of the tone noise mechanism over laminar airfoils. Journal of Fluid Mechanics. 2007 Nov 25;591:155.

[14] Nash EC, Lowson MV, McAlpine A. Boundary-layer instability noise on aerofoils. Journal of Fluid Mechanics. 1999 Mar;382:27-61.

[15] Paterson RW, Vogt PG, Fink MR, Munch CL. Vortex noise of isolated airfoils. Journal of Aircraft. 1973 May;10(5):296-302.

[16] Chen E, Ma Y, Yang A, Zhao G. Experimental investigation on noise emissions of an airfoil with non-flat plate trailing edge serrations. Journal of Mechanical Science and Technology. 2019 Jul;33(7):3069-74.

[17] Moreau DJ, Doolan CJ. Noise-reduction mechanism of a flat-plate serrated trailing edge. AIAA journal. 2013 Oct;51(10):2513-22.